ORIGINAL ARTICLE

Characterization of glycine-*N*-acyltransferase like 1 (GLYATL1) in prostate cancer

Marie-Lisa Eich MD[1] | Darshan Shimoga Chandrashekar PhD[1] |
Maria Del Carmen Rodriguez Peña MD[1] | Alyncia D. Robinson MS[1] | Javed Siddiqui MS[2] |
Stephanie Daignault-Newton MS[3] | Balabhadrapatruni V. S. K. Chakravarthi PhD[1] |
Lakshmi Priya Kunju MD[2] | George J. Netto MD[1] | Sooryanarayana Varambally PhD[1,4]

[1]Department of Pathology, The University of Alabama at Birmingham, Birmingham, Alabama

[2]Department of Pathology, The University of Michigan, Ann Arbor, Michigan

[3]Department of Biostatistics, The University of Michigan, Ann Arbor, Michigan

[4]O'Neal Comprehensive Cancer Center, University of Alabama at Birmingham, Birmingham, Alabama

Correspondence
George J. Netto, Department of Pathology, The University of Alabama at Birmingham, WP Bld, Suite P230 l 619 19th St, South, Birmingham, AL 35249-7331.
Email: gnetto@uabmc.edu

Sooryanarayana Varambally, Department of Pathology, The University of Alabama at Birmingham, WTI Building, Suite l, Birmingham, AL 35249-7331.
Email: svarambally@uabmc.edu

Abstract

Background: Recent microarray and sequencing studies of prostate cancer showed multiple molecular alterations during cancer progression. It is critical to evaluate these molecular changes to identify new biomarkers and targets. We performed analysis of glycine-*N*-acyltransferase like 1 (GLYATL1) expression in various stages of prostate cancer in this study and evaluated the regulation of GLYATL1 by androgen.

Method: We performed in silico analysis of cancer gene expression profiling and transcriptome sequencing to evaluate GLYATL1 expression in prostate cancer. Furthermore, we performed immunohistochemistry using specific GLYATL1 antibody using high-density prostate cancer tissue microarray containing primary and metastatic prostate cancer. We also tested the regulation of GLYATL1 expression by androgen and ETS transcription factor ETV1. In addition, we performed RNA-sequencing of GLYATL1 modulated prostate cancer cells to evaluate the gene expression and changes in molecular pathways.

Results: Our in silico analysis of cancer gene expression profiling and transcriptome sequencing we revealed an overexpression of GLYATL1 in primary prostate cancer. Confirming these findings by immunohistochemistry, we show that GLYATL1 is overexpressed in primary prostate cancer compared with metastatic prostate cancer and benign prostatic tissue. Low-grade cancers had higher GLYATL1 expression compared to high-grade prostate tumors. Our studies showed that GLYATL1 is upregulated upon androgen treatment in LNCaP prostate cancer cells which harbors ETV1 gene rearrangement. Furthermore, ETV1 knockdown in LNCaP cells showed downregulation of GLYATL1 suggesting potential regulation of GLYATL1 by ETS transcription factor ETV1. Transcriptome sequencing using the GLYATL1 knockdown prostate cancer cell lines LNCaP showed regulation of multiple metabolic pathways.

Conclusions: In summary, our study characterizes the expression of GLYATL1 in prostate cancer and explores the regulation of its regulation in prostate cancer showing role for androgen and ETS transcription factor ETV1. Future studies are needed to decipher the biological significance of these findings.

KEYWORDS

androgen, ETV1, GLYATL1, immunohistochemistry, prostate cancer

1 | INTRODUCTION

Prostate cancer (PCa) is the most prevalent cancer entity in men with an estimated 174 650 new cases in 2019 in the USA. Despite recent advances in diagnosis and treatment, it remains the second most cancer-related cause of death.[1] Recent molecular studies have paved the way to a better understanding of the underlying biology of tumor growth and progression. This offers new possibilities to find new therapeutic targets for the disease.[2,3]

GLYATL1 encodes an enzyme that catalyzes arylacetyl transfer.[4,5] In noncancerous tissue it was found to be highly expressed in liver and kidney, and to a lesser extent in pancreas, testis, ovary and stomach.[6] Human glycine *N*-acyltransferases (GLYATL, GLYATL1, GLYATL2, and GLYATL3) are involved in conjugation of carboxylic acids to glycine and glutamine. This conjugation is thought to be a part of a pathway for the detoxification of benzoate and other xenobiotics.[7] GLYAT plays a major role in liver metabolism. It regulates mitochondrial adenosine triphosphate (ATP) production, glycine availability, CoASH (Coenzyme A) availability and the detoxification of various organic acids.[7-9] Human GLYATL2 conjugates medium- and long-chain saturated and unsaturated acyl-CoA esters to glycine producing *N*-oleoyl glycine and *N*-arachidonoyl glycine. The latter are structurally and functionally related to endocannabinoids and have been identified as signaling molecules that regulate functions such as the perception of pain and body temperature. They have also been found to have anti-inflammatory properties.[10] Furthermore, GLYATL2 was found to be a target of ETS transcription factor ETV1, which is along with other ETS transcription factors rearranged in ~50% of human prostate cancer cases.[11,12]

Microarray studies have shown that in breast cancer, *GLYATL1* was among genes differently expressed in the contralateral unaffected breast in women with estrogen-receptor-negative compared with those with estrogen-receptor positive breast cancer.[13] In prostate cancer cell lines GLYATL1 was shown to play a role in colony forming ability.[14] To date, its expression in cancerous tissue and its role in tumorigenesis is not well understood.

In this study, we sought to analyze the expression and regulation of GLYATL1 in prostate cancer. Our investigation suggests that GLYATL1 is overexpressed in low-grade disease. Furthermore, we show that androgen treatment and ETS transcription factor ETV1 plays a role in regulating its expression.

2 | MATERIALS AND METHODS

2.1 | Gene expression from the Cancer Genome Atlas

Gene expression levels of *GLYATL1* in normal prostate and prostate adenocarcinoma were interrogated utilizing UALCAN (http://ualcan.path.uab.edu), a web portal providing the Cancer Genome Atlas (TCGA) RNA sequencing data in the form of boxplots, depicting gene expression levels.[15]

2.2 | Prostate tissue samples

Benign and prostate cancer tissues were obtained from radical prostatectomy series and from the Rapid Autopsy Program at the University of Michigan through appropriate informed consent. Institutional Review Board approval was obtained to procure and analyze the tissues. Two tissue microarrays including 134 patients were constructed with a total of 321 TMA spots.

2.3 | Immunohistochemistry

Immunohistochemistry (IHC) was carried out to evaluate GLYATL1 expression using rabbit polyclonal antibody against GLYATL1 (catalog #HPA039501, 1:200; Sigma-Aldrich, MO). Formalin-fixed, paraffin-embedded tissue sections were deparaffinized and rehydrated. Antigen retrieval was performed by boiling the slides for 10 minutes in citrate buffer (catalog #C9999-1000ML; Sigma-Aldrich). Immunostaining was performed using the Vector Laboratories staining kit following the manufacturer's protocol. Endogenous peroxidase activity was blocked using BLOXALL Blocking Solution (catalog #SP-6000; Vector Laboratories). Nonspecific binding sites were blocked by incubation with normal horse serum (R.T.U., 2.5%, catalog #S-2012; Vector Laboratories). Primary antibody was added in a 1:200 dilution for 1.5 hours at room temperature according to dilution protocol optimized in our laboratory. After washing with phosphate buffer saline (PBS), secondary antibody (anti-rabbit, catalog #MP-7401; Vector Laboratories) was added for 45 minutes at room temperature. Following two washings (5 minutes each) with PBS and PBS-T, antibody signals were detected using ImmPACT DAB (catalog #SK-4105; Vector Laboratories). Hematoxylin QS (catalog # H-3404; Vector Laboratories) was used as a counterstain. Sections were then dehydrated.

2.4 | Immunohistochemical scoring system

GLYATL1 IHC expression was evaluated by a genitourinary pathologist. The scoring system consisted of a modified quantitative H-score system (ranging from 0 to 300) in which GLYATL1 expression was estimated as the products of the intensity (0 for negative, 1 for weakly positive, 2 for moderately positive, and 3 for strongly positive) multiplied by the extent of the staining in the tumor cells (0% to

100%). GLYATL1 score is reported by diagnosis and by Gleason score. Each sample core was plotted with multiple cores per patient. The mean, 95% confidence intervals, and pairwise t test P values reported were adjusted for the correlation among multiple samples per patient using a clustered analysis. The analysis for Figure 3 was generated using SAS software. Copyright© 2016 SAS Institute Inc, SAS and all other SAS Institute Inc, product or service names are registered trademarks or trademarks of SAS Institute Inc, Cary, NC, USA.
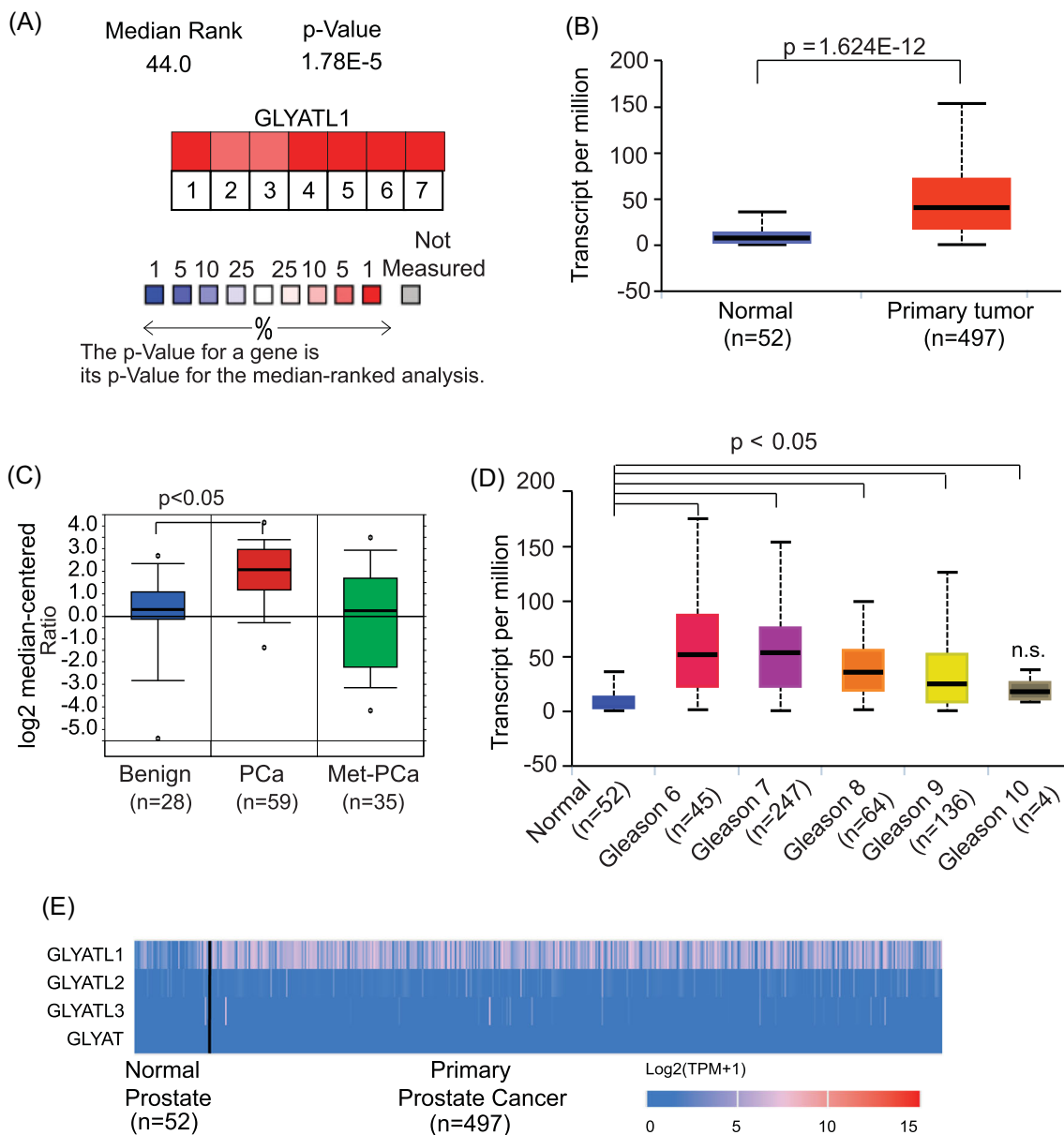

FIGURE 1 The human *N*-acytransferase GLYATL1 shows increased expression in prostate cancer. A, Gene expression profiling analysis of multiple prostate cancer datasets using Oncomine database shows higher GLYATL1 expression in primary prostate cancer compared with benign prostate tissue across the datasets (The rank for a gene is the median rank for that gene across each of the analyses. The *P* value for a gene is its *P* value for the median ranked analysis). B, Transcriptome sequencing of prostate cancer. GLYATL1 expression in benign, primary, and metastatic prostate cancer were measured in transcript per million utilizing the TCGA Data set. C, Expression of GLYATL1 in normal prostate, primary and metastatic tumor samples using the data set by Grasso et al. D, GLYATL1 expression analysis per Gleason score utilizing the TCGA data set. E, Expression of the human glycine *N*-acyltransferases (GLYATL1, GLYATL2, GLYATL3, and GLYAT) in primary prostate cancer and normal prostate tissue. GLYATL1, glycine-*N*-acyltransferase like 1; PCa, prostate cancer [Color figure can be viewed at wileyonlinelibrary.com]
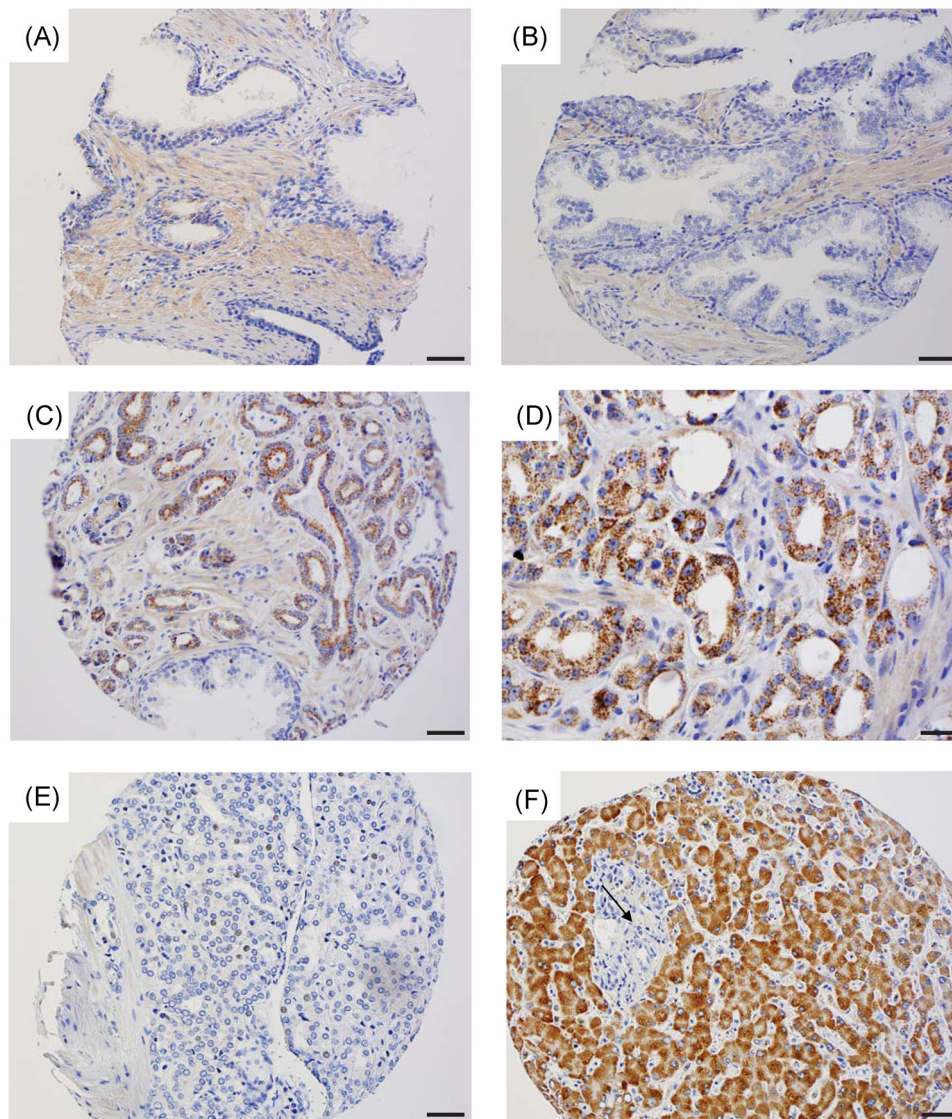
FIGURE 2 Immunohistochemical staining of GLYATL1 in prostate. A, benign prostate tissue; B, high-grade prostatic intraepithelial neoplasia; C, D, Gleason score 6 prostate cancer; E, Gleason score 8 prostate cancer; F, liver metastasis of prostate cancer (arrow) showing low or no staining of GLYATL1. Scale bars = 50 μm in (A, B, C, E, and F); 20 μm in (D). GLYATL1, glycine-*N*-acyltransferase like 1 [Color figure can be viewed at wileyonlinelibrary.com]

2.5 | Western blot analyses

For Western blot analysis, protein samples were, as previously described,[16] separated on sodium dodecyl sulfate polyacrylamide gel electrophoresis (4-12%; Invitrogen). Equal amounts of proteins were loaded and transferred for 2 hours at 0.35A onto an Immobilon1-P polyvinylidene fluoride (PVDF) membrane (EMD Millipore, Billerica, MA). To block nonspecific binding, the membrane was incubated for 1 hour in blocking buffer (Tris-buffered saline, 0.1% Tween 20 [TBS-T], 5% nonfat dry milk) followed by incubation overnight at 4°C with the primary antibody. After two washes with TBS-T for 5 minutes, the blot was incubated with horseradish peroxidase-conjugated secondary antibody (1:5000) for 1 hour at room temperature. The membrane was again washed with TBS-T and TBS twice for 5 minutes each

and signals were visualized by Luminata Crescendo chemiluminescence Western blot analysis substrate as per manufacturer's protocol (EMD Millipore). For loading control β-actin was applied. Therefore the membrane was incubated, after two washes with TBS-T, with the anti-β-actin antibody for 1 hour at room temperature. After again two washings with TBS-T and TBS signals were visualized, as described above, using Luminata Crescendo chemiluminescence Western blot analysis substrate as per manufacturer's protocol (EMD Millipore). Antibodies used in the study are anti-GLYATL1 (catalog # HPA039501, 1:1000; Sigma-Aldrich), anti-PSA rabbit polyclonal antibody (Dako Denmark A/S 1:1000; Dako), anti-HRP-β-actin (catalog # HRP-60008, 1:20 000; PTG Labs, Rosemont, IL), anti-rabbit IgG HRP (catalog # SA00001-2, 1:5000; PTG Labs, Rosemont). All antibodies were employed at dilutions optimized in our laboratory.
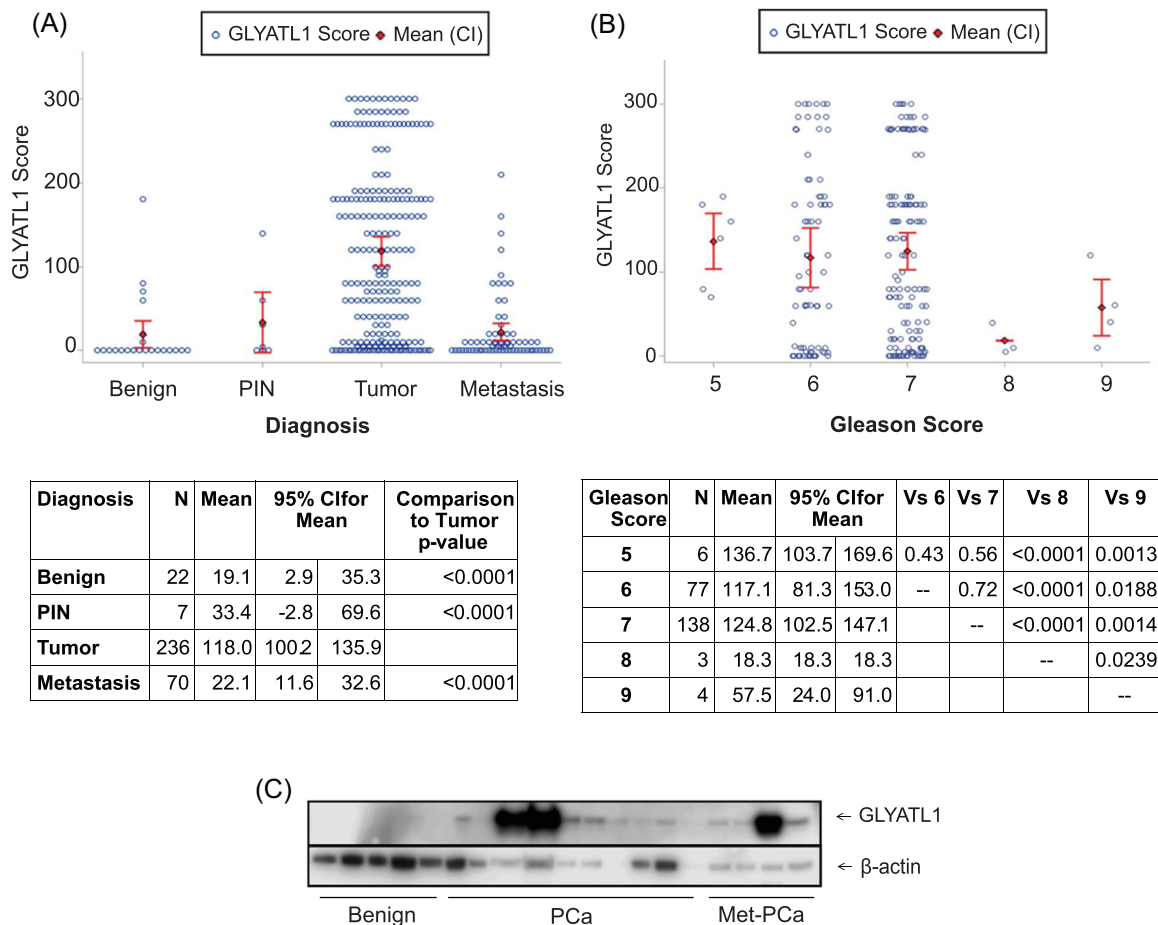
FIGURE 3 Higher expression of GLYATL1 in primary prostate cancer. A, Immunohistochemical score of GLYATL1 in benign prostate tissue, high-grade prostatic intraepithelial (PIN), primary tumors and metastasis. B, analysis of GLYATL1 immunohistochemical score in primary prostate cancer per Gleason score. C, Western Blot analysis of GLYATL1 using benign prostate tissue, primary and metastatic prostate cancer samples. GLYATL1, glycine-N-acyltransferase like 1 [Color figure can be viewed at wileyonlinelibrary.com]

2.6 | Cell culture

Human prostate cancer cell lines LNCaP, C4-2B, 22Rv1, PC3, DU145, and VCaP, as well as RWPE-1, were obtained from ATCC. LNCaP, C4-2B, 22Rv1, PC3 and DU145 cells were cultivated at 37°C in RPMI medium (Gibco RPMI 1640 Medium [+] L-Glutamine, Life Technologies) supplemented with 10% fetal bovine serum and 100 U/mL penicillin G and 100 μg/mL streptomycin in a humidified environment with 5% CO_2. VCaP cells were cultivated at 37°C in Dulbecco Modified Eagle's medium + GlutaMAX (Gibco DMEM(1×) + GlutaMAX, Life Technologies) supplemented with 10% fetal bovine serum and 100 U/mL penicillin G and 100 μg/mL streptomycin (Life Technologies) in a humidified environment with 5% CO_2. RWPE-1 cells were cultivated in Keratinocyte Serum Free Medium (Gibco Life Technologies) supplemented with 2.5 μg EGF (Gibco Life Technologies) and 25 mg Bovine Pituitary Extract (Life Technologies) and 100 U/mL penicillin G and 100 μg/mL streptomycin (Life Technologies) in a humidified environment with 5% CO_2. Normal prostate epithelial cells (PrEC) were obtained from Clonetics Corporation (San Diego, CA) and were maintained in prostate epithelial cell medium (PrEGM) supplemented with a mixture of various growth factors (SingleQuots) (Clonetics); and 10% fetal bovine serum.

2.7 | GLYATL1 and ETV1 knockdown in prostate cancer cells

ETV1 and nontargeting small interfering RNA (siRNA) were obtained from Dharmacon, (Lafayette, CO) and transfection experiments were performed followed the manufacturer's protocol. For transfection Lipofectamine RNAi MAX reagent (Thermo Fisher) was applied. Cells were seeded $1 × 10^5$ in a six-well plate and simultaneously transfected with siRNA. Twenty-four hours later a second identical transfection was performed. Cells were harvested 72 hours after the first transfection for RNA isolations and Western blot experiments. siRNA used in this study are shown in Table ST1.

Stable knockdowns were created using short hairpin RNA (shRNA) purchased from SBI (System Biosciences, Mountain View, CA; see Table ST2). Lentiviruses for creating these stable knockdowns were created by the University of Alabama at Birmingham

Vector Core. After infection of prostate cells with lentiviruses expressing GLYATL1 shRNA or nontargeting shRNA, stable knockdown cell lines were generated by selection with 1 µg/mL puromycin (Life Technologies).

2.8 | RNA extraction and real-time polymerase chain reaction

Total RNA from prostate cancer cells was extracted by using Directzol RNA MiniPrep Plus kit (Zymo Research) according to the manufacturer's protocol. RNA from tissue was harvested by employing the Qiagen RNAeasy kit. Each sample was transcribed into complementary DNA (cDNA) by using Superscript III Reverse Transcriptase (ThermoFischer Scientific), deoxynucleoside triphosphates, and random hexamer primers (ThermoFischer Scientific). For each real-time polymerase chain reaction (RT-PCR) amplification, 2 µL of cDNA (200 ng/µL) product, 5 µL SYBR green PCR Master Mix (Applied Biosystems), 1 µL primer solution, and 2 µL of DNAse/RNAse free water was added for a final volume of 10 µL. Thermocylcling conditions were as suggested by the manufacturer: 95° for 20 seconds to activate the polymerase followed by 40 cycles of 95° for 15 seconds and 60° for 1 minute. SYBR green was used to determine the messenger RNA (mRNA) expression level of a gene of interest. Levels were normalized to beta-Actin using the $\Delta\Delta C_t$ method. All primers for SYBR green were synthesized by Integrated DNA Technologies (Coralville, IA) and listed in Table ST3. All PCRs were performed in triplicates.

2.9 | Transcriptome sequencing analyses

RNA from prostate cancer cells (22Rv1 and LNCaP) treated with GLYATL1 shRNA and nontargeting shRNA were sequenced using Illumina sequencer. The raw sequence reads obtained as FASTQ files were trimmed using Trim Galore (v0.4.1) (http://www.bioinformatics.babraham.ac.uk/projects/trim_galore/) to remove adapter sequences and low-quality reads. After performing the quality control analysis using FastQC (v0.11.5) (http://www.bioinformatics.babraham.ac.uk/projects/fastqc/), the trimmed reads were mapped to the human genome (GRCh38/hg38) using TopHat v2.1.0.[17] The aligned reads were sorted via samtools (Version: 1.3.1).[18] HTSeq-count (version 0.6.0)[19] was used to obtain raw read counts for each annotated human gene. Differential expression analysis between GLYATL1 shRNA and nontargeting shRNA treated samples was carried out using DESeq[20] considering "blind" method for estimating dispersion and "fit-only" sharing mode. Genes with an absolute fold change of 1.5 or more and $P < .05$ were considered as differentially expressed [DEG]. Gene ontology and Kyoto Encyclopedia of Genes and Genomes (KEGG) pathway enrichment analysis on differentially expressed genes were performed using online platform DAVID (Database for Annotation, Visualization, and Integrated Discovery) version 6.8.[21] Volcano plots and heatmap were generated in R 3.2.2 (https://cran.r-project.org/) using gplots package [https://cran.r-project.org/web/packages/gplots/index.html].

2.10 | Accession numbers

The RNA sequencing data are submitted to the Gene Expression Omnibus (GEO) database, www.ncbi.nlm.nih.gov/geo (accession no. GSE130395).

2.11 | ChIP sequencing and promoter analyses

AR binding in the GLYATL1 promoter region in prostate cancer cells (LNCaP) treated with dihydrotestosterone (DHT) was explored. SRA files corresponding to GSE83860[22] and GSE92347[23] were downloaded. Table S4 shows a complete list of raw data downloaded and processed. Downloaded SRA files were converted to FASTQ files using SRA Toolkit (https://www.ncbi.nlm.nih.gov/sra/docs/toolkitsoft/). ChIP-seq raw data were processed as mentioned in Chakravarthi et al.[24] The upstream region of GLYATL1 and KLK3 (as positive control) was explored for AR binding using Integrative Genome Viewer (IGV).[25]

AR peak sequence located within GLYATL1 promoter region was extracted, and scanned for AR position weight matrix (PWM) (MA0007.2) using JASPAR database.[26] Details of AR ChIP-seq raw data files downloaded from NCBI Sequence Read Archive (SRA) database are shown in Table ST4.

2.12 | Statistical analysis

GLYATL1 expression index (EI) from tissue microarrays was reported by tissue diagnosis and Gleason score separately. Expression index equals the intensity expression score multiplied by the percent of cells displaying the expression. Each sample core was plotted with multiple cores per patient. The mean, 95% confidence intervals, and pairwise t test P values reported were adjusted for the correlation among multiple samples per patient using a clustered analysis. The statistical analysis of the tissue microarray immunohistochemistry data was generated using SAS software. Copyright© 2016 SAS Institute Inc. SAS and all other SAS Institute Inc. product or service names are registered trademarks or trademarks of SAS Institute Inc, Cary, NC, USA.

Statistical analysis for cell proliferation study was performed by using JMP® 13.1.0. To determine significant differences between two groups, the Wilcoxon rank sum test was applied for continuous variables. $P < .05$ were considered significant.

3 | RESULTS

3.1 | GLYATL1 is overexpressed in low grade and localized prostate cancer

Based on our in silico analysis of publicly available prostate cancer gene expression data using the Oncomine database (Oncomine Platform; Life Technologies, Ann Arbor, MI)[27] we found GLYATL1 to be overexpressed in human prostate adenocarcinomas in seven independent gene expression profiling studies (Figure 1A)

(P = 1.78E−5).[28-33] By applying the Oncomine database and the web portal UALCAN[15] it could be shown that *GLYATL1* was significantly overexpressed in human prostate cancer compared to benign prostate tissue in the study by Lapointe et al[31] (See Figure S1A) and the TCGA study cohort[2] (P = 1.624E−12) (Figure 1B). The in silico analysis of the study by Grasso et al revealed an overexpression of *GLYATL1* in primary prostate cancer compared to benign tissue and metastatic tumors (Figure 1C). Furthermore, *GLYATL1* was especially overexpressed in the lower grade tumors in the TCGA study cohort (Figure 1D). Looking at the three other Human Glycine N-acyltransferases (*GLYATL2*, *GLYATL3*, and *GLYAT*) revealed that the observed overexpression in prostate cancer was unique for *GLYATL1* (Figure 1E).

3.2 | Immunohistochemical and Western blot analyses of GLYATL1 in prostate cancer tissue

Using a GLYATL1 specific antibody, we performed immunohisto-chemistry staining on TMAs containing benign prostatic tissue, prostatic intraepithelial neoplasia (PIN), localized and metastatic prostate cancer. Representative staining patterns are depicted in Figure 2. The arrow in the Figure 2F shows the prostate cancer liver metastasis showing the absence of GLYATL1 expression. TMA analyses showed an increased GLYATL1 protein expression in line with our in silico analysis of GLYATL1 mRNA. GLYATL1 is over-expressed especially in localized prostate tumors compared to normal prostatic tissue (P < .0001), PIN (<.0001) and metastatic prostate cancer (P < .0001) (Figure 3A and 3B). Analyses of a subset of prostatic adenocarcinomas based on grade showed a higher GLYATL1 expression in Gleason score 5, 6, and 7 tumors compared with those with Gleason score 8 and 9. Furthermore, Western Blot experiments revealed that GLYATL1 protein was present primarily in localized prostate cancer and metastases, and it was not detectable in benign tissue (Figure 3C).

3.3 | GLYATL1 expression is regulated by androgen and ETV1

RT-PCR (Figure 4A) and Western blot analysis (Figure 4B) displayed that GLYATL1 is expressed in the androgen receptor (AR) containing prostate cancer cell lines LNCaP, C4-2B, 22Rv1, and VCaP. It was absent in prostate epithelial cells and RWPE-1 (resembling cells of benign prostatic hyperplasia), as well as PC3 and DU145, which lack androgen receptor expression. After treating LNCaP with 5 nM Methyltrienolone (R1881) and 10 nM DHT for 48 hours, levels of GLYATL1 mRNA were increased compared with GLYATL1 levels in nontreated or vehicle-control cells (Figure 4C). Similarly, mRNA expression levels of the androgen-regulated gene prostate-specific antigen (PSA) were increased (Figure 4D). Western blot analysis showed similar results (Figure 4E). Analyses of AR ChIP-seq data in DHT treated LNCaP revealed AR occupancy in the *GLYATL1* promoter region (Figure 4F, Figure S2B), indicating GLYATL1 as an

AR target. Furthermore, GLYATL1 was decreased upon ETV1 knockdown in LNCaP cells (Figure 4G).

3.4 | Molecular pathways altered by GLYATL1 modulation in prostate cancer cells

To investigate the signaling events that are regulated by GLYATL1, we performed GLYATL1 knockdown using a specific shRNA targeting *GLYATL1* in prostate cancer cell lines LNCaP and 22Rv1. The knockdown in LNCaP was confirmed by RT-PCR and Western blot (Figure 5B). Transcriptome sequencing was performed using RNA from GLYATL1 knockdown (GLYATL1 shRNA) as well as control cells. Figure 5A shows the top 40 up- and downregulated genes upon GLYATL1 knockdown in LNCaP cells. Our analysis identified that upon GLYALT1 knockdown, 164 protein-coding genes were down-regulated and 105 protein-coding genes were upregulated (Figure 5C). Table S5 and S6 provide the up and downregulated genes in 22Rv1 and LNCaP cells after GLYATL1 knockdown. Table S7 and S8 provide the biological processes and KEGG pathways altered upon GLYATL1 knockdown in these cells. KEGG pathways enriched in differentially expressed genes on GLYATL1 knockdown includes glycolysis and gluconeogenesis as well as hypoxia-inducible factor 1 (HIF-1) signaling, metabolic pathways and central carbon metabolism in cancer (Figure 5D).

Knockdown confirmation, top up- and downregulated genes, as well as KEGG pathways enriched after GLYATL1 knockdown in 22Rv1 are shown in Figure S1B-SD.

4 | DISCUSSION

In this study, we evaluated the expression and regulation of Glycine-N-Acyltransferase Like 1 in prostate cancer. GLYATL1 as an enzyme, involved in *N*-acyl amino acid production and metabolism, is normally expressed in liver and kidney.[6,7] Microarray studies have shown its overexpression in prostate cancer.[5,14,34,35] Our in silico analysis further indicates, GLYATL1 transcripts to be higher in localized prostate cancers compared with benign prostatic tissue and meta-static prostate cancer. Especially the lower Gleason grade tumors (≤7) showed a high GLYATL1 expression. This was further confirmed by Western blot analysis and immunohistochemistry, showing GLYATL1 protein expression to be low in benign prostate tissue, PIN and most of the metastatic prostate cancers.

To evaluate the potential role of GLYATL1 in prostate cancer, we analyzed its expression in prostate cancer cell lines. In their study on next-generation RNAseq in castration-resistant prostate cancer cell lines, Ma et al[36] found GLYATL1 among the top 8 downregulated genes in PC3 and DU145 (which represent acquired resistance to androgens) vs LNCaP cells. In line with that, we found GLYATL1 to be present in prostate cancer cell lines that express AR (LNCaP, C4-2B, VCaP, and 22Rv1) and absent in DU145, PC3, benign prostate epithelial cells and RWPE-1. Our analyses further identified that GLYATL1 expression is induced by androgen treatment in LNCaP
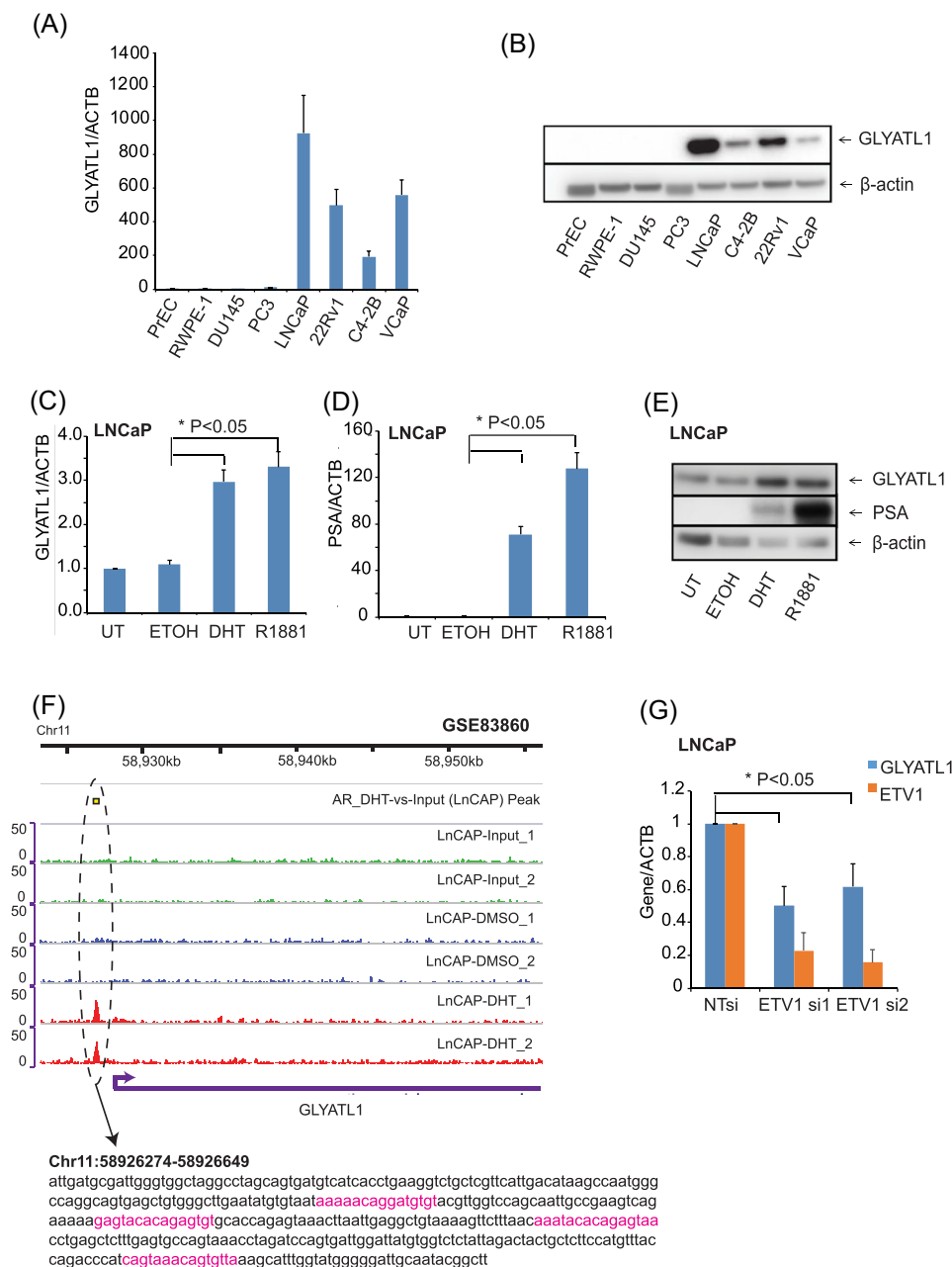
FIGURE 4 GLYATL1 expression is regulated by androgen and ETV1. A, B, Western blot analysis and quantitative reverse transcription polymerase chain reaction analysis of GLYATL1 in prostate cancer cell lines. C, D, GLYATL1 and prostate-specific antigen (PSA) mRNA expression in untreated, vehicle control treated (ethanol [ETOH]), and androgen-treated (dihydrotestosterone [DHT], methyltrienolone [R1881]) LNCaP cells. E, Western blot analysis of GLYATL1 in androgen-treated LNCaP cells. F, IGV output representing the gene neighborhood region of GLYATL1, showing AR ChIP-seq peaks in the proximal promoter region in LNCaP cells treated with dihydrotestosterone. AR ChIP-seq data from Malinen et al[22] (GSE83860) were used. Peaks annotated using Homer shown in the topmost lane. AR peak sequence (Chr11:58926274-58926649) with AR consensus (highlighted in the pink font) shown below. G, GLYATL1 expression in ETV1 knockdown LNCaP cells. GLYATL1, glycine-N-acyltransferase like 1 [Color figure can be viewed at wileyonlinelibrary.com]

cells. ChIP-Seq data analyses showed AR binding in the promoter region of the *GLYATL1* gene, emphasizing a direct regulation of GLYATL1 by androgen signaling. As prostate cancer growth is initially androgen-dependent, the gold-standard treatment option for advanced disease is androgen deprivation.[37] However, most

patients eventually develop resistance and disease progression. Thus, several studies have investigated signaling events that lead to castration-resistant prostate cancer (CRPC).[30,38,39] Kaushik et al[38] have recently shown, that glucosamine-phosphate N-acetyltransferase 1, an enzyme involved in the hexosamine biosynthetic pathway,
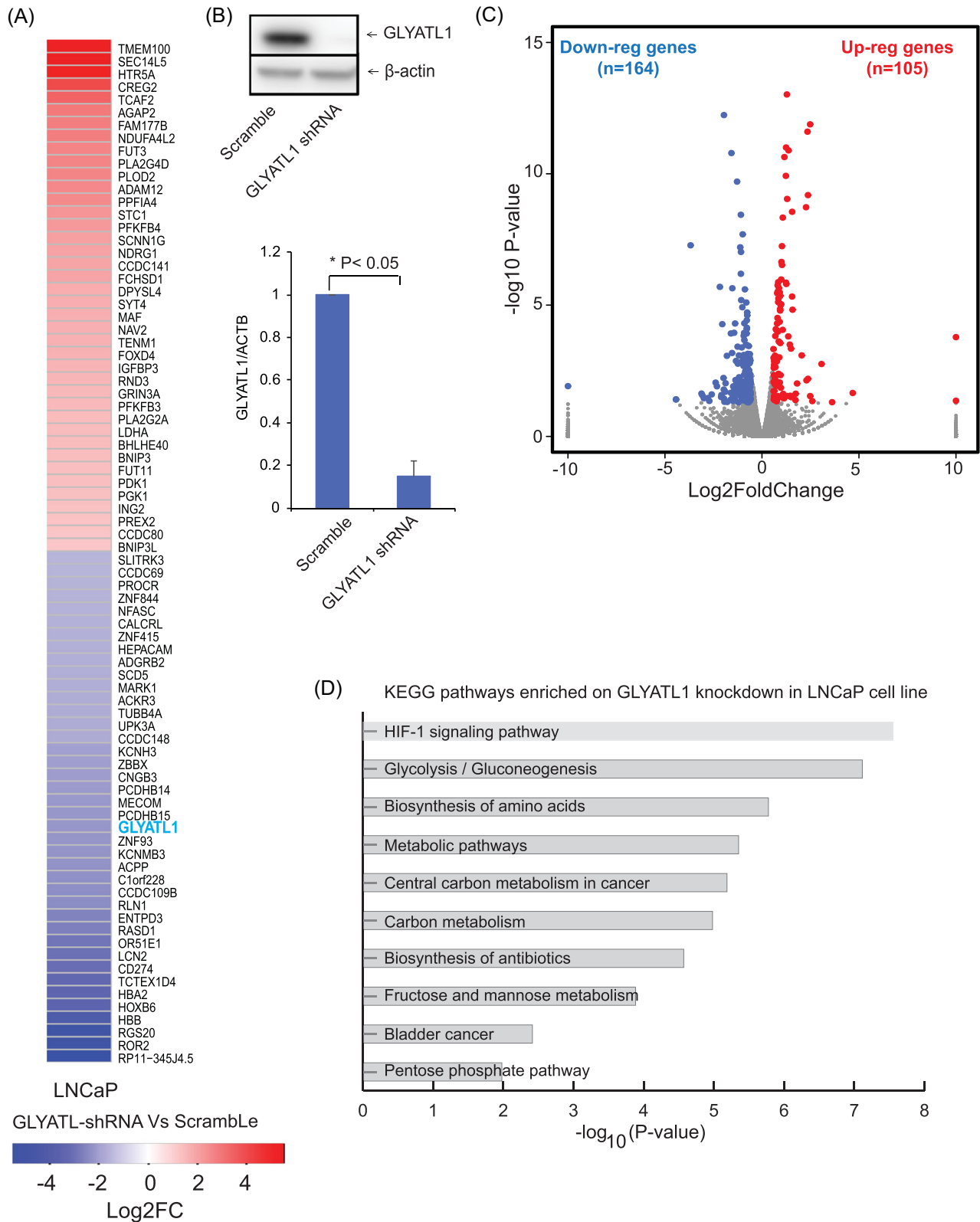
FIGURE 5 RNA sequencing analysis of GLYATL1 knockdown in LNCaP cells. A, Heatmap showing top 40 up- and downregulated genes after GLYATL1 knockdown in LNCaP cells. B, Western blot analysis and real-time polymerase chain reaction confirmation of GLYATL1 knockdown in LNCaP cells. C, Volcano plot showing distribution of differentially expressed genes on GLYATL1 knockdown in LNCaP cells. Log2 fold change is represented in *x*-axis, while *y* axis represents −log10 *P* value. Gene upregulated are marked with red dots, while blue dots indicate genes downregulated. D, Bar plot showing top 10 KEGG pathways enriched in genes differentially expressed on GLYATL1 knockdown in LNCaP cell line. GLYATL1, glycine-*N*-acyltransferase like 1 [Color figure can be viewed at wileyonlinelibrary.com]

is significantly decreased in CRPC compared with localized prostate cancer. Similarly, we found GLYATL1 to be lower in metastatic prostate cancer. Whether this expression pattern has a role for GLYATL1 in the development of CRPC remains to be investigated.

As mentioned above, chromosomal rearrangements involving ETS transcription factors, such as ERG and ETV1, are the most frequent alterations in prostate cancer. Translocations place the coding regions of the latter mentioned genes under the control of androgen-responsive promoters, such as *TMPRSS2*.[40] ETV1 expression in ETV1 knock-in mice was found to positively cooperate with AR signaling, leading to additional enhancement of expression of AR targets.[41] In line with this mechanism, we found GLYATL1 not only to be upregulated upon androgen treatment, but also downregulated in LNCaP cells following ETV1 knockdown, indicating a potential regulatory role for this ETS transcription factor in GLYATL1 expression.

Serum level of PSA is a widely used screening biomarker.[42] However, PSA elevation is not very specific for prostate cancer, as numerous benign conditions, like benign prostatic hyperplasia, can cause a rise in its serum levels. Therefore, there is a need for additional risk stratification. In this setting, urine as a liquid biopsy platform is actively being investigated. In a study by Leyten et al[35] GLYATL1, along with 15 other biomarkers, was described to be differentially expressed in urine sediments from prostate cancer patients compared to healthy controls. This further emphasizes GLYATL1's potential as an early stage biomarker.

To understand the pathways that may be regulated by GLYATL1, we performed RNA sequencing using shRNA specifically targeting GLYATL1 in prostate cancer cell lines. Pathway analysis in LNCaP GLYATL1 knockdown cells revealed a potential involvement in metabolic pathways including glycolysis. Anaerobic glycolysis has been shown to be one of the main metabolic changes in CRPC-like cells.[43] Whether GLYATL1 knockdown could be similarly implicated in driving LNCaP cells towards a more aggressive phenotype will require further assessment and could then provide a rational for our finding of lower GLYATL1 levels in metastatic tumors compared to localized prostate cancers.

In summary, our study further characterizes the expression GLYATL1 in prostate cancer and explores its regulation. We show GLYATL1 overexpression mainly in low grade and localized prostate cancer. Additionally, our findings indicate that androgen and ETV1 are involved in its regulation. Future studies are needed to decipher the biological significance of these findings.

CONFLICT OF INTERESTS

The authors declare that there are no conflict of interests.

ORCID

Sooryanarayana Varambally 🆔 http://orcid.org/0000-0002-2277-1127

REFERENCES

1. Siegel RL, Miller KD, Jemal A. Cancer statistics, 2019. *CA Cancer J Clin.* 2019;69:7-34.
2. Abeshouse A, Ahn J, Akbani R, et al. The molecular taxonomy of primary prostate cancer. *Cell.* 2015;163:1011-1025.
3. Chakravarthi BV, Nepal S, Varambally S. Genomic and epigenomic alterations in cancer. *Am J Pathol.* 2016;186:1724-1735.
4. Matsuo M, Terai K, Kameda N, et al. Designation of enzyme activity of glycine-*N*-acyltransferase family genes and depression of glycine-*N*-acyltransferase in human hepatocellular carcinoma. *Biochem Biophys Res Commun.* 2012;420:901-906.
5. Barfeld SJ, East P, Zuber V, Mills IG. Meta-analysis of prostate cancer gene expression data identifies a novel discriminatory signature enriched for glycosylating enzymes. *BMC Med Genomics.* 2014;7:513.
6. Zhang H, Lang Q, Li J, et al. Molecular cloning and characterization of a novel human glycine-*N*-acyltransferase gene GLYATL1, which activates transcriptional activity of HSE pathway. *Int J Mol Sci.* 2007;8:433-444.
7. van der Sluis R, Badenhorst CP, Erasmus E, van Dyk E, van der Westhuizen FH, van Dijk AA. Conservation of the coding regions of the glycine *N*-acyltransferase gene further suggests that glycine conjugation is an essential detoxification pathway. *Gene.* 2015;571:126-134.
8. Badenhorst CP, Erasmus E, van der Sluis R, Nortje C, van Dijk AA. A new perspective on the importance of glycine conjugation in the metabolism of aromatic acids. *Drug Metab Rev.* 2014;46:343-361.
9. Badenhorst CPS, van der Sluis R, Erasmus E, van Dijk AA. Glycine conjugation: importance in metabolism, the role of glycine *N*-acyltransferase, and factors that influence interindividual variation. *Expert Opin Drug Metab Toxicol.* 2013;9:1139-1153.
10. Waluk DP, Sucharski F, Sipos L, Silberring J, Hunt MC. Reversible lysine acetylation regulates activity of human glycine *N*-acyltransferase-like 2 (hGLYATL2): implications for production of glycine-conjugated signaling molecules. *J Biol Chem.* 2012;287:16158-16167.
11. Paulo P, Ribeiro FR, Santos J, et al. Molecular subtyping of primary prostate cancer reveals specific and shared target genes of different ETS rearrangements. *Neoplasia.* 2012;14:600-611.
12. Tomlins SA, Rhodes DR, Perner S, et al. Recurrent fusion of TMPRSS2 and ETS transcription factor genes in prostate cancer. *Science.* 2005;310:644-648.
13. Wang J, Shidfar A, Ivancic D, et al. Overexpression of lipid metabolism genes and PBX1 in the contralateral breasts of women with estrogen receptor-negative breast cancer. *Int J Cancer.* 2017;140:2484-2497.
14. Nalla AK, Williams TF, Collins CP, Rae DT, Trobridge GD. Lentiviral vector-mediated insertional mutagenesis screen identifies genes that influence androgen independent prostate cancer progression and predict clinical outcome. *Mol Carcinog.* 2016;55:1761-1771.
15. Chandrashekar DS, Bashel B, Balasubramanya SAH, et al. UALCAN: a portal for facilitating tumor subgroup gene expression and survival analyses. *Neoplasia.* 2017;19:649-658.

16. Chakravarthi BV, Goswami MT, Pathi SS, et al. Expression and role of PAICS, a De Novo purine biosynthetic gene in prostate cancer. *Prostate*. 2017;77:10-21.

17. Kim D, Pertea G, Trapnell C, Pimentel H, Kelley R, Salzberg SL. TopHat2: accurate alignment of transcriptomes in the presence of insertions, deletions and gene fusions. *Genome Biol*. 2013;14:R36.

18. Li H. A statistical framework for SNP calling, mutation discovery, association mapping and population genetical parameter estimation from sequencing data. *Bioinformatics*. 2011;27:2987-2993.

19. Anders S, Pyl PT, Huber W. HTSeq—a Python framework to work with high-throughput sequencing data. *Bioinformatics*. 2015;31: 166-169.

20. Anders S, Huber W. Differential expression analysis for sequence count data. *Genome Biol*. 2010;11:R106.

21. Huang da W, Sherman BT, Lempicki RA. Systematic and integrative analysis of large gene lists using DAVID bioinformatics resources. *Nat Protoc*. 2009;4:44-57.

22. Malinen M, Niskanen EA, Kaikkonen MU, Palvimo JJ. Crosstalk between androgen and pro-inflammatory signaling remodels androgen receptor and NF-kappaB cistrome to reprogram the prostate cancer cell transcriptome. *Nucleic Acids Res*. 2017;45:619-630.

23. Chattopadhyay I, Wang J, Qin M, et al. Src promotes castration-recurrent prostate cancer through androgen receptor-dependent canonical and non-canonical transcriptional signatures. *Oncotarget*. 2017;8:10324-10347.

24. Chakravarthi B, Chandrashekar DS, Hodigere Balasubramanya SA, et al. Wnt receptor Frizzled 8 is a target of ERG in prostate cancer. *Prostate*. 2018;78:1311-1320.

25. Robinson JT, Thorvaldsdottir H, Winckler W, et al. Integrative genomics viewer. *Nat Biotechnol*. 2011;29:24-26.

26. Khan A, Fornes O, Stigliani A, et al. JASPAR 2018: update of the open-access database of transcription factor binding profiles and its web framework. *Nucleic Acids Res*. 2018;46:D260-D266.

27. Rhodes DR, Kalyana-Sundaram S, Mahavisno V, et al. Oncomine 3.0: genes, pathways, and networks in a collection of 18,000 cancer gene expression profiles. *Neoplasia*. 2007;9:166-180.

28. Varambally S, Yu J, Laxman B, et al. Integrative genomic and proteomic analysis of prostate cancer reveals signatures of metastatic progression. *Cancer Cell*. 2005;8:393-406.

29. Arredouani MS, Lu B, Bhasin M, et al. Identification of the transcription factor single-minded homologue 2 as a potential biomarker and immunotherapy target in prostate cancer. *Clin Cancer Res*. 2009;15:5794-5802.

30. Grasso CS, Wu Y-M, Robinson DR, et al. The mutational landscape of lethal castration-resistant prostate cancer. *Nature*. 2012;487: 239-243.

31. Lapointe J, Li C, Higgins JP, et al. Gene expression profiling identifies clinically relevant subtypes of prostate cancer. *Proc Natl Acad Sci USA*. 2004;101:811-816.

32. Taylor BS, Schultz N, Hieronymus H, et al. Integrative genomic profiling of human prostate cancer. *Cancer Cell*. 2010;18:11-22.

33. Vanaja DK, Cheville JC, Iturria SJ, Young CY. Transcriptional silencing of zinc finger protein 185 identified by expression profiling is associated with prostate cancer progression. *Cancer Res*. 2003;63: 3877-3882.

34. Arencibia JM, Martin S, Perez-Rodriguez FJ, Bonnin A. Gene expression profiling reveals overexpression of TSPAN13 in prostate cancer. *Int J Oncol*. 2009;34:457-463.

35. Leyten GH, Hessels D, Smit FP, et al. Identification of a candidate gene panel for the early diagnosis of prostate cancer. *Clin Cancer Res*. 2015;21:3061-3070.

36. Ma Y, Miao Y, Peng Z, et al. Identification of mutations, gene expression changes and fusion transcripts by whole transcriptome RNAseq in docetaxel resistant prostate cancer cells. *SpringerPlus*. 2016;5:1861.

37. Network NCC. National Comprehensive Cancer Network (NCCN): Prostate Cancer. 2018.

38. Kaushik AK, Shojaie A, Panzitt K, et al. Inhibition of the hexosamine biosynthetic pathway promotes castration-resistant prostate cancer. *Nat Commun*. 2016;7:11612.

39. Waltering KK, Urbanucci A, Visakorpi T. Androgen receptor (AR) aberrations in castration-resistant prostate cancer. *Mol Cell Endocrinol*. 2012;360:38-43.

40. Tomlins SA, Mehra R, Rhodes DR, et al. Integrative molecular concept modeling of prostate cancer progression. *Nature Genet*. 2007;39: 41-51.

41. Baena E, Shao Z, Linn DE, et al. ETV1 directs androgen metabolism and confers aggressive prostate cancer in targeted mice and patients. *Genes Dev*. 2013;27:683-698.

42. Schroder FH, Hugosson J, Roobol MJ, et al. Screening and prostate cancer mortality: results of the European Randomised Study of Screening for Prostate Cancer (ERSPC) at 13 years of follow-up. *Lancet*. 2014;384:2027-2035.

43. Shafi AA, Putluri V, Arnold JM, et al. Differential regulation of metabolic pathways by androgen receptor (AR) and its constitutively active splice variant, AR-V7, in prostate cancer cells. *Oncotarget*. 2015;6:31997-32012.

SUPPORTING INFORMATION

Additional supporting information may be found online in the Supporting Information section.